Green, J. R., and Westley, J. (1961), *J. Biol. Chem. 236,* 3047.
Horowitz, P., and DeToma, F. (1970), *J. Biol. Chem. 245,* 984.
Jarabak, R., and Westley, J. (1974a), *Biochemistry 13,* 3233.
Jarabak, R., and Westley, J. (1974b), *Biochemistry 13,* 3237.
King, E. L., and Altman, C. (1956), *J. Phys. Chem. 60,* 1375.
Olive, C., Geroch, M. E., and Levy, H. R. (1971), *J. Biol. Chem. 246,* 2047.
Rudolph, F. B., and Fromm, H. J. (1970), *Biochemistry 9,* 4660.
Westley, J., and Heyse, D. (1971), *J. Biol. Chem. 246,* 1468.
Westley, J., and Nakamoto, T. (1962), *J. Biol. Chem. 237,* 547.
Wong, J. T., and Hanes, C. S. (1962), *Can. J. Biochem. Physiol. 40,* 763.

Different Expressions of Cooperativity in the Kinetics of Two Forms of Cytoplasmic Malic Dehydrogenase†

David Vetterlein and Marvin Cassman*

ABSTRACT: Initial rate kinetics were carried out on two forms of cytoplasmic malic dehydrogenase (S-MDH *a* and *b*). Nonhyperbolic kinetics were observed with NADH and oxaloacetate as substrates using S-MDH *b*, while the double-reciprocal plots for S-MDH *a* showed marked deviations from linearity with NAD^+ and L-malate, and only slight curvature with oxaloacetate as substrate. In all cases, the departure from linearity in the double reciprocal plots was dependent on the concentration of cosubstrate. The two forms of S-MDH had essentially identical values of V_{max} in the direction of NAD^+ reduction, but S-MDH *a* had a maximum rate of NADH oxidation approximately threefold higher than S-MDH *b*. The kinetic behavior of these enzymes cannot be uniquely defined in terms of a given molecular mechanism. However, the kinetics, together with previous physical and structural studies, were consistent with a physiological role for S-MDH in regulating the oxidation of glycolytic NADH.

Metabolic regulation on the enzyme level is generally indicated by the presence of allosteric interactions. The term "allosteric" was initially defined as indirect interactions between distinct binding sites (Monod *et al.*, 1965). Operationally, the phenomena which characterizes an allosteric protein are (1) a change in the apparent affinity, or in the Michaelis constant, with changing fractional saturation of a ligand ("cooperativity"); and (2) a change in the apparent affinity, or in the Michaelis constant, of one ligand by the presence or absence of a second, structurally unrelated, ligand ("allosteric modifier"). Although the nature of the molecular mechanism(s) which generate these phenomena is of considerable interest in understanding the relation of structure and function in proteins, the physiological significance of allosteric behavior is independent of its molecular genesis. The importance of allostery in metabolic regulation was further emphasized by the discovery that enzymes could exist in two chemically distinct, stable forms having different allosteric properties. In several cases, these forms could be shown to be interconvertible by cellular processes involving chemical modification of the proteins (Holzer and Duntze, 1971). In effect, this process of covalent modification adds another element to metabolic control mechanisms, allowing given enzymes to function with or without superimposed allosteric constraints.

In our earlier studies we had demonstrated that cytoplasmic malic dehydrogenase (S-MDH),[1] isolated from beef heart, could exist in two stable enzyme forms (S-MDH *a* and *b*) with different regulatory properties (Cassman and King, 1972; Cassman, 1973; Cassman and Vetterlein, 1974). S-MDH *b* showed cooperative binding and kinetics with respect to NADH, and exhibited allosteric inhibition of NADH binding by fructose 1,6-bisphosphate. S-MDH *a* was catalytically more active, and showed no allosteric interactions with NADH. S-MDH *a* contained 1.3–1.8 mol of trichloroacetic acid precipitable phosphate/mol of enzyme, while S-MDH *b* contained 0.3–0.6 mol of phosphate/mol of enzyme.

In this paper, detailed kinetic studies are reported which indicate that S-MDH *a* and *b* show striking differences in their overall kinetic behavior, and that both forms interact cooperatively with substrates other than NADH. The results are discussed in terms of a proposed role for the two enzyme forms in regulating the mode of reoxidation of glycolytic NADH.

Materials and Methods

Materials

NADH, NAD^+, oxaloacetate, and L-malate were all A grade, from Calbiochem. All other chemicals were standard reagent grade.

Both forms of cytoplasmic malic dehydrogenase were prepared from beef heart by the method of Guha *et al.* (1968). The enzyme preparations were characterized as S-MDH *a* and *b* using the criteria described previously (Cassman and Vetterlein, 1974). Phosphate content appears to be the best quantitative criterion for determining the amount of each enzyme form in a given preparation. Based on analysis of several different preparations, it was assumed that S-MDH *a* has 2 mol of phosphate/mol of enzyme, and S-MDH *b* 0 mol of phosphate/mol of enzyme (Cassman and Vetterlein, 1974). The enzymes used in the work reported here had 1.85 mol of phosphate/mol of S-MDH *a*, and 0.17 mol of phosphate/mol of S-MDH *b*. Be-

† From the Section of Biochemistry and Molecular Biology, Department of Biological Sciences, University of California, Santa Barbara, California 93106. *Received November 26, 1973.* This research was supported by Faculty Grant 547 of the University of California.

[1] Abbreviation used is: S-MDH, cytoplasmic malic dehydrogenase.

cause of limitations on the amount of material available for analysis, the standard errors for these values cannot be determined. The values obtained suggest there is at most a 10% heterogeneity in the samples used.

The factors which affect the appearance of the two enzyme forms in a given preparation are not yet clearly understood. Either S-MDH *a* or *b* may be obtained from a single beef heart, with heterogeneity within a sample with respect to the two enzyme forms not exceeding 30% (Cassman and Vetterlein, 1974).

Kinetic Measurements. All measurements of reaction rates were performed with a Hitachi Perkin-Elmer MPF-2A fluorescence spectrometer, equipped with a thermostated cell holder. The temperature was kept constant at 21–22°, using a circulating water bath.

The rates of NADH oxidation or NAD^+ reduction were measured by following the change in NADH fluorescence emission at 460 nm upon excitation at 340 nm. The NADH fluorescence was calibrated with a series of NADH solutions of known concentrations, which had been diluted from a stock solution. The dependence of fluorescent intensity on NADH concentration was linear over the concentration range used.

All measurements were performed in 3-ml volumes, and 1-cm path-length cells. Slit widths were kept fixed at a 6-nm half-bandwidth. Measurement of initial rates were begun within 20 sec after addition of the enzyme, and the change in fluorescence intensity was monitored on a strip-chart recorder. The slopes were linear for at least the first minute of measurement.

Experiments were carried out in sodium–potassium phosphate buffer, pH 6.0, ionic strength = 0.05. Reagents and enzyme dilutions were made fresh each day. The enzyme was diluted into a buffer solution containing 0.1% serum albumin, and checked during the course of the day for losses in activity. Enzyme concentrations in the assay were $1–4 \times 10^{-10}$ M. In addition, the stock solution of enzyme was also assayed periodically, using the standard assay conditions previously described (Cassman and Vetterlein, 1974). NADH and oxaloacetate were prepared in pH 7.5 buffer and added to the reaction mixture in microliter volumes using Eppendorf micropipets. The reaction mixture after addition was pH 6.0. Assays were performed immediately after the reactants were prepared, and measurements were made during the course of the day under standard conditions to check for decomposition. In addition, the fluorescence yield of NADH aliquots was determined periodically to ensure that it remained constant.

NADH concentrations were determined by measuring the optical density at 340 nm, and applying the extinction coefficient $\epsilon_{340\,nm}^{1\,cm} = 6.22 \times 10^3\ M^{-1}\ cm^{-1}$ (Horecker and Kornberg, 1949). NAD^+ was determined spectrophotometrically after enzymatic reduction with alcohol dehydrogenase. L-Malate was assayed enzymatically in a reaction mixture containing, in a total volume of 2.9 ml, 300 nmol of glycine–NaOH buffer (pH 10.5), 1.0 mmol of semicarbazide, 15 μmol of NAD^+, and excess malic dehydrogenase. Oxaloacetate was assayed enzymatically with malic dehydrogenase and an excess of NADH.

Data Analysis. Reciprocal plots of the kinetic data were fit, where possible, to either a linear or quadratic function. The program used was a standard polynomial regression analysis from the University of California, Los Angeles, Biomedical Computer Program series. The determination of which function gave the best fit to the data was based on both a minimum variance in the fit, and a random scatter of the experimental points around the fitted curve.

Errors in plots of kinetic data were generated primarily by errors in the measurement of reaction rates, since substrate concentrations could be determined with a high degree of accuracy. The major source of error was therefore the accuracy with which the slopes of the recorder plots can be evaluated. The spectrofluorometer offers a considerable advantage in this respect, owing to the flexibility in changing the scale of the recorder, by altering photomultiplier sensitivity. Through making such adjustments, the per cent standard deviations in the reciprocal plots were kept to 3–6% over most of the concentrations used. Exceptions to this occurred at some of the lowest velocities measured. Error bars are therefore given in the figures only for the replots of slopes or intercepts. In general, each point was repeated two to three times, with some of the lowest rates being repeated four to five times.

Results

Kinetic Measurements of the Reaction in the Direction of NAD^+ Reduction. Previous studies had shown that the two forms of S-MDH isolated from beef heart exhibited striking differences in the kinetics and binding of NADH (Cassman and Vetterlein, 1974). Preliminary investigations had also indicated that these differences, although noticeable at high pH, were most marked at pH 6, while at lower pH the enzyme became relatively unstable (M. Cassman, unpublished results). As a consequence, the detailed kinetic measurements reported here were all performed at pH 6. Analysis at this pH entails particular difficulties in studies with malic dehydrogenase, owing to the effect of hydrogen ions on the equilibrium for the reaction. The equilibrium for reaction 1 lies far in the direction

$$\text{L-malate} + NAD^+ \rightleftharpoons \text{oxaloacetate} + NADH + H^+ \quad (1)$$

of NADH oxidation at pH 6, with an equilibrium constant of 3.43×10^{-6} (Burton and Wilson, 1953). To obtain initial rates of NAD^+ reduction, measurements must therefore be made when only small amounts of the substrates have been reacted. The fluorimetric assay, under the conditions used, was capable of detecting changes in NADH concentration of as little as 5×10^{-10} M. At the lowest concentrations of NAD^+ and L-malate assayed, this represented less than 0.4% of the concentration change to equilibrium. It was therefore possible to determine initial velocities from linear regions of the curve recording NADH changes with time. The measured rates were linear for at least 1 min, and were linear with enzyme concentration over about a 10-fold concentration range of enzyme.

Double-reciprocal plots of velocity with varying NAD^+ and L-malate were obtained using S-MDH *b*. The experimental points could all be fit by a linear regression with a high degree of accuracy. The replots of slopes and intercepts *vs.* the reciprocal of the fixed substrate concentrations were linear, as expected.

These results correspond to a rate equation having the form

$$\frac{1}{v} = \frac{1}{V_m} + \frac{K_{NAD}}{V_m}\frac{1}{\{NAD\}} + \frac{K_{Mal}}{V_m}\frac{1}{\{Mal\}} + \frac{K_{NM}}{V_m}\frac{1}{\{NAD\}}\frac{1}{\{Mal\}} \quad (2)$$

where the terms in brackets are molar substrate concentrations and K_{NAD} and K_{Mal} are Michaelis constants. For two-substrate reactions, they represent the substrate concentration giving half-maximal velocity at saturating concentrations of the second substrate. V_m is the maximum velocity at saturating concentrations of both substrates, and K_{NM} is the complex constant defined by Alberty (1953). The values of the constants were obtained from the replots of slopes and intercepts (Dalziel, 1957; Cleland, 1970) and are given in Table I.

TABLE I: Kinetic Parameters For S-MDH *a* and *b*.[a]

	S-MDH *a*	S-MDH *b*
V_{max} (NAD^+/malate)[b]	8.77 ± 0.5	7.54 ± 0.07
K_{NAD^+}	$7.6 \pm 0.6 \times 10^{-5}$	$3.35 \pm 0.5 \times 10^{-5}$
K_{malate}	(8.6×10^{-5})[c]	$2.78 \pm 0.4 \times 10^{-5}$
K_{NM}[d]		$2.59 \pm 0.1 \times 10^{-8}$
V_{max} (NADH/oxaloacetate)[b]	278 ± 30	(94.3 ± 5)[e]
K_{NADH}	$1.79 \pm 0.07 \times 10^{-6}$	$(1.54 \pm 0.2 \times 10^{-6})$[e]
$K_{oxaloacetate}$	$2.26 \pm 0.2 \times 10^{-6}$	
K_{NO}[d]	$3.2 \pm 5.0 \times 10^{-16}$	

[a] The Michaelis constants for L-malate and NAD^+, using S-MDH *b*, are independent of the concentration of cosubstrate. The Michaelis constants for all other substrates are those obtained at saturating concentrations of cosubstrate. [b] Given in units of μmol/min per mg of protein. [c] Obtained from the slope of the kinetic plot at a fixed concentration of $NAD^+ = 1 \times 10^{-3}$ M (Figure 2). [d] K_{NM} and K_{NO} are the complex constants defined by Alberty (1953), in the direction of NAD^+ reduction and NADH oxidation, respectively. [e] Obtained from the kinetic plot made at a fixed concentration of oxaloacetate $= 4.35 \times 10^{-5}$ M (Figure 4).

It should be noted that eq 2 is not applicable to subsequent studies, since the appearance of nonlinear double-reciprocal plots indicates that the interaction terms in eq 2 cannot be treated as constants. Values of the interaction terms for such plots are presented when linear replots of limiting slopes or intercepts are generated, and reflect *only* the limiting conditions as substrate concentrations approach saturation. They have therefore only operational significance, and do not reflect any mechanistic assumptions.

Reciprocal plots have also been generated for varying NAD^+ and L-malate using S-MDH *a* (Figures 1 and 2). In contrast to the data obtained with S-MDH *b*, the points in Figures 1 and 2 could not be fit by a linear regression over the entire range of concentrations examined. Further, the deviation from linearity in these plots was dependent on the concentration of fixed substrate. To obtain a quantitative estimate of the degree of curvature of the plots with L-malate as variable substrate, the Hill coefficient was calculated, using

$$\log\left(\frac{V}{V_m} - 1\right) = j \log \frac{1}{\{S\}} - \log \frac{1}{K} \qquad (3)$$

where v = measured reaction rate, V_m = maximum velocity at concentration of fixed substrate used, $\{S\}$ = variable substrate concentration, and j = Hill coefficient (Cleland, 1970; Whitehead, 1970). (K is an empirical constant whose value is not required for this analysis.) V_m, the extrapolated ordinate intercept, was obtained from the polynomial used to fit the experimental points. It should be stressed that the significance of the Hill coefficient is intended to be limited to an empirical index of the departure of the kinetic plots from linearity. No mechanistic model is implied.

Only the first four concentration points were used to fit the lines showing upward curvature (Figure 1), since the rates at the lowest concentrations used had a substantially greater standard deviation than the other measured values, and tended to bias the shape of the curve.

Values of the calculated Hill coefficients at different fixed NAD^+ concentrations are given in Table II. At the three lowest NAD^+ concentrations used, the Hill coefficients were es-

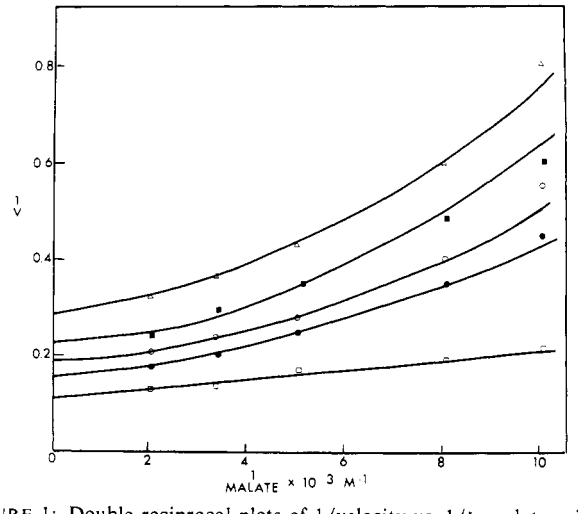

FIGURE 1: Double-reciprocal plots of 1/velocity *vs.* 1/L-malate using S-MDH *a*, at varying fixed NAD^+ concentrations. The lines represent measurements done at △, 5×10^{-5} M; ■, 7.5×10^{-5} M; ○, 1.25×10^{-4} M; ●, 2.04×10^{-4} M; □, 1×10^{-3} M. The units of reciprocal velocity on the ordinate are $(\mu mol/min \text{ per mg enzyme})^{-1}$. In this and all subsequent figures, the rates were measured at pH 6, in sodium-potassium phosphate buffer, ionic strength = 0.05. Unless noted otherwise, the lines represent the least-squares fit to the experimental points (see Methods).

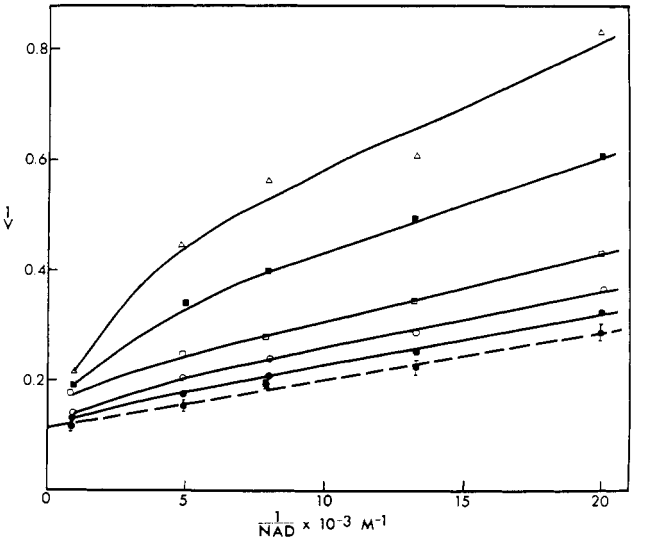

FIGURE 2: Double-reciprocal plots of 1/velocity *vs.* $1/NAD^+$ using S-MDH *a*, at varying fixed L-malate concentrations. The dashed line is the replot of the ordinate intercepts of Figure 1, *i.e.*, at extrapolated infinite concentration of L-malate. The bars are the calculated standard deviations of the intercepts. The other lines represent fixed concentrations of L-malate of △, 1×10^{-4} M; ■, 1.25×10^{-4} M; □, 2×10^{-4} M; ○, 3×10^{-4} M; ●, 5×10^{-4} M. The replot of intercepts is fitted by least-squares line. All other experimental points had the lines fitted by eye. The units of reciprocal velocity on the ordinate are $(\mu mol/min \text{ per mg enzyme})^{-1}$.

TABLE II: Hill Coefficients from Nonlinear Kinetic Plots at Different Fixed Concentrations of Cosubstrate.[a]

S-MDH *a*				S-MDH *b*	
NAD^+ Concn (M)	Hill Coef Varying L-Malate (Figure 1)	NADH Concn (M)	Hill Coef Varying Oxaloacetate (Figure 3)	Oxaloacetate Concn (M)	Hill Coef Varying NADH (Figure 4)
1×10^{-3}	1.00	2.0×10^{-6}	1.11	4.35×10^{-5}	0.98
2×10^{-4}	1.43	1.2×10^{-6}	1.10	3.48×10^{-6}	1.16
1.25×10^{-4}	1.70	4.8×10^{-7}	1.18	1.74×10^{-6}	1.21
7.5×10^{-5}	1.75	3.0×10^{-7}	1.52	6.09×10^{-7}	1.01
5×10^{-5}	1.68			2.6×10^{-7}	1.02

[a] The Hill coefficients were calculated as described in the text. The log–log plots were linear over the concentrations of variable substrate used. The average errors in the Hill coefficients were ±0.03.

sentially identical at 1.71 ± 0.03, and reach a value of 1.0 at the highest NAD^+ concentration. Since the Hill coefficients were nearly invariant at the lowest NAD^+ concentrations, this indicates that the apparent K_{Mal} is remaining constant in this range, and thus the linearity of the reciprocal plots at low varying NAD^+ concentrations (Figure 2) is understandable.

To obtain an estimate of K_{NAD} at saturating L-malate concentration, the extrapolated ordinate intercepts of Figure 1 were replotted against the fixed NAD^+ concentrations. This replot is shown as the dashed line in Figure 2. The values for K_{NAD} and for V_m, taken from the ordinate intercept of the replot, are given in Table I. Errors in measurement of the slopes were too great to permit evaluation of the complex constant K_{NM}.

Because the downward curvature of the plots with varying NAD^+ was entirely determined by one point, it was hazardous to attempt an extrapolation to the ordinate intercept. For the same reason, no attempt was made to fit the points in Figure 2 with a regression line. Rather, an approximate value for K_{Mal} was obtained from the kinetic plot determined at a fixed

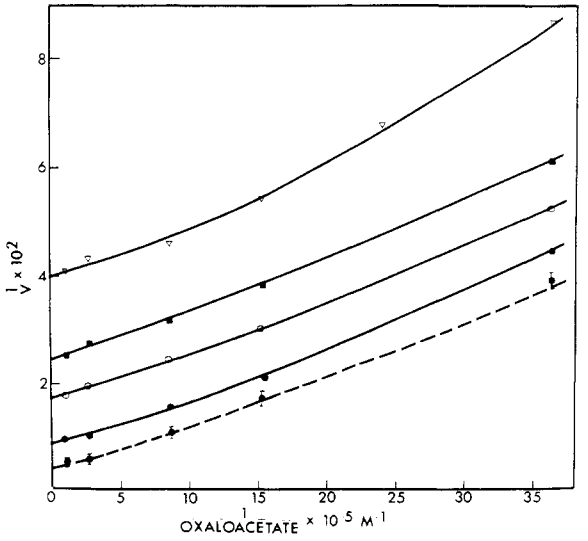

FIGURE 3: Double-reciprocal plots of 1/velocity *vs.* 1/oxaloacetate using S-MDH *a*, at varying fixed concentrations of NADH. The dashed line is a replot of the extrapolated ordinate intercepts from a plot of 1/velocity *vs.* 1/NADH, *i.e.*, at extrapolated infinite concentration of NADH. The bars are calculated standard deviations of the intercepts. The other lines represent fixed concentrations of NADH of ▽, 1.72×10^{-7} M; ■, 3×10^{-7} M; ○, 4.8×10^{-7} M; ●, 1.2×10^{-6} M. The units of reciprocal velocity on the ordinate are (μmol/min per mg of enzyme)$^{-1}$.

NAD^+ concentration of 1×10^{-3} (Figure 1). This concentration of NAD^+ is approximately 14 times higher than the value determined for K_{NAD}.

It is interesting to note that, despite the considerable qualitative differences in the curvature of the reciprocal plots, S-MDH *a* and *b* have Michaelis constants for NAD^+ and L-malate which differ by only twofold. The maximal velocities were essentially identical.

Kinetic Studies of the Reaction in the Direction of NADH Oxidation. Measurements of initial velocities were also made for both S-MDH *a* and *b* with oxaloacetate and NADH as variable substances. Since there is evidence that oxaloacetate interacts with the enzyme as the keto form (Loewus *et al.*, 1955), it was necessary to correct the total oxaloacetate concentration to obtain the concentration of the keto acid. At pH 6, the enol form appears to comprise 13% of the total (Loewus *et al.*, 1955; Dolin, 1968). All of the concentrations given for oxaloacetate are therefore equal to 0.87 × [total oxaloacetate]. It was also necessary that the rate of the reaction be sufficiently slow, so that the rate of the keto–enol tautomerization was not rate limiting. Dolin (1968) has calculated the maximum rate compatible with this requirement to be 0.3–0.35 μmol of oxaloacetate converted per min per μmol of oxaloacetate. Since the maximum rate in our system was 0.09 μmol of oxaloacetate reduced per min per μmol of oxaloacetate, this condition was therefore fulfilled.

Plots of reciprocal velocity *vs.* reciprocal NADH and oxaloacetate concentrations were obtained for S-MDH *a*. The plots with NADH as variable substrate could all be fitted with linear regression lines. In contrast, the plots with varying oxaloacetate appear to show upward curvature (Figure 3). Although the curvature was rather slight, the small standard deviations justified utilizing a nonlinear regression line as a fit. Furthermore, there appeared to be no undetermined systematic error biasing the velocities at low oxaloacetate concentrations, since a similar curvature was not observed with S-MDH *b* (see below). However, it is possible that the small degree of curvature observed is due to an error in the estimate of the amount of keto form present.

Replots of slopes and intercepts were made, and the calculated kinetics constants are given in Table I. All the replots were linear, except for the curve representing the rates extrapolated to saturating levels of NADH (shown as the dashed line in Figure 3). As expected, this plot showed a shallow upward curvature. It is possible, however, that at sufficiently high NADH concentrations, the linearity of the plots with varying NADH and the nonlinearity of the plots with varying oxaloa-

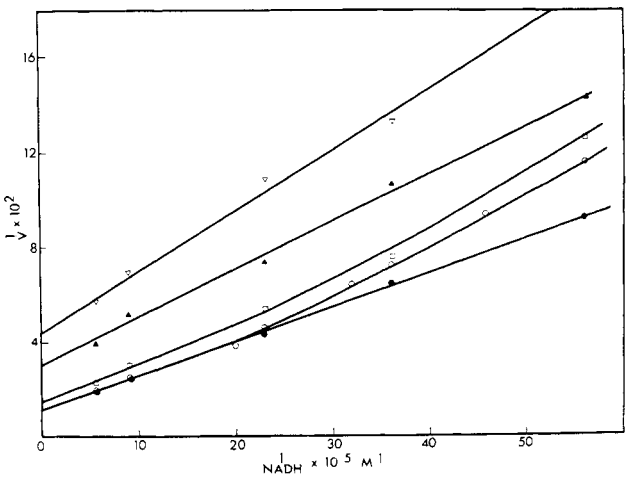

FIGURE 4: Double-reciprocal plots of 1/velocity *vs.* 1/NADH using S-MDH *b*, at varying fixed concentrations of oxaloacetate: ▽, 2.6×10^{-7} M; ▲, 6.1×10^{-7} M; □, 1.74×10^{-6} M; ○, 3.4×10^{-6} M; ●, 4.35×10^{-5} M. The units of reciprocal velocity on the ordinate are (μmol/min per mg of enzyme)$^{-1}$.

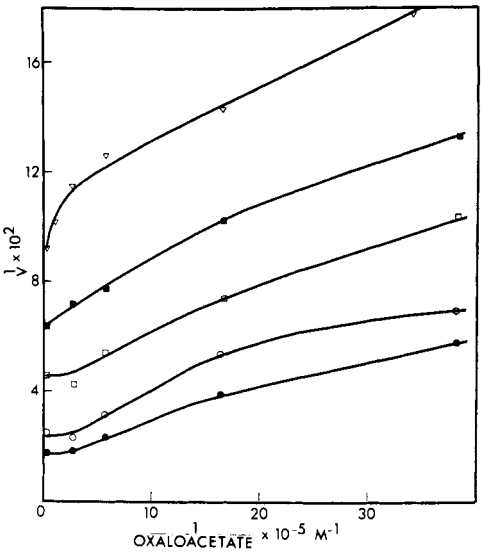

FIGURE 5: Double-reciprocal plot of 1/velocity *vs.* 1/oxaloacetate using S-MDH *b*, at varying fixed NADH concentrations: ▽, 1.8×10^{-7} M; ■, 2.8×10^{-7} M; □, 4.35×10^{-7} M; ○, 1.08×10^{-6} M; ●, 1.8×10^{-6} M. All lines were fit by eye to the experimental points. The units of reciprocal velocity on the ordinate are (μmol/min per mg of enzyme)$^{-1}$.

cetate would both disappear, analogous to the behavior of this enxyme form with NAD^+ and L-malate as substrates. The dependence of the Hill coefficients for the oxaloacetate plots on NADH concentration was in fact quite similar to the effects observed with NAD^+ and L-malate. Thus, the Hill coefficients for the kinetics with oxaloacetate as variable substrate go from 1.15 ± 0.05 to 1.52 with decreasing NADH concentration (Table II).

Reciprocal plots were obtained for S-MDH *b*, and a comparison with S-MDH *a* demonstrated even more striking qualitative differences than was observed for the reaction in the direction of NAD^+ reduction. When NADH is the variable substrate (Figure 4), the points were fitted by a linear regression at the two lowest fixed oxaloacetate concentrations, showed upward curvature at the next two highest concentrations, and were again linear at the highest fixed oxaloacetate concentration. The corresponding plot with oxaloacetate as variable substrate was even more unusual (Figure 5). In this case, the plots determined at the three highest fixed NADH concentrations were biphasic, first showing a curvature concave to the abscissa, and then apparently reaching a plateau or approaching some minimum slope. At the two lowest NADH concentrations, the curves appear to be monotonic, showing only downward curvature. No attempt was made to obtain a least-squares fit to the points in Figure 5, and the lines shown were drawn by eye. The nature of the curvature of the plots in Figures 4 and 5 did not seem to justify any attempt to obtain replots. However, the convergence of the plots obtained at the two highest fixed oxaloacetate concentrations (Figure 4) allowed us to calculate an approximate value for the maximum velocity, and for the Michaelis constant for NADH (Table I).

Discussion

Recent studies have provided evidence that malic dehydrogenase can be isolated from beef heart in two functionally distinguishable forms. The two forms, termed S-MDH *a* and *b*, were differentiated by several criteria. S-MDH *b* had a lower specific activity in the direction of NADH oxidation, compared to S-MDH *a*. In addition, S-MDH *b* displayed cooperative kinetics and a protein concentration dependence with respect to NADH binding (Cassman and King, 1972), and was allosterically inhibited by fructose 1,6-bisphosphate (Cassman, 1973). None of these properties were exhibited by S-MDH *a* (Cassman and Vetterlein, 1974). Structurally, the two forms had identical amino acid compositions and subunit molecular weights. They both appeared to have a dimer of mol wt 77,000 as the maximum degree of polymerization. However, S-MDH *a* contained 1.3–1.6 mol of trichloroacetic acid precipitable phosphate/mol of enzyme, compared to 0.3–0.6 mol/mol of S-MDH *b* (Cassman and Vetterlein, 1974). The detailed kinetic studies described in this paper were initiated with the purpose of determining the differences between the two enzymes, in their interaction with substrates in the catalytic process. Such studies might then provide further evidence about the nature of the mechanisms involved in interaction with substrates, as well as the physiological role of SMDH *a* and *b*.

Initial rate measurements, performed at pH 6, demonstrated that the differences between S-MDH *a* and *b* in their interaction with substrate were not limited to NADH. Further, deviations from linearity in the double-reciprocal plots were observed in both enzymes with substrates other than NADH. Nonlinear plots can be obtained from solutions containing more than one enzyme catalyzing the same reaction. If the two enzymes have rate equations that can be expressed in the form of eq 2, an equimolar mixture of enzymes differing 10-fold in V_m and K_m will still generate only a slight downward curvature (Plowman, 1972). It seems, therefore, that the very complex kinetics described above can hardly be due to heterogeneity, particularly since the preparations used were at most 10% heterogeneous with respect to the two enzyme forms (see Materials).

The presence of upward or downward curvature is frequently taken as an indication of positive or negative cooperativity, respectively. This designation of "cooperative" behavior should be considered only as an empirical description which indicates a change in the apparent Michaelis constant with changing substrate concentration. Particularly for two-substrate enzymes, there are a number of mechanisms which have been proposed to explain the appearance of nonlinearity in kinetic double-reciprocal plots (Monod *et al.*, 1965; Koshland *et al.*, 1966; Frieden, 1967; Sweeney and Fisher, 1968). The available evidence to support one or another of these models will be presented later.

The deviation from Michaelis–Menten kinetics of an enzyme

system can be quantitated by determining the Hill coefficient (Cleland, 1970). In the direction of NAD^+ reduction, the Hill coefficients for the kinetic data using S-MDH *b* was 0.98 ± 0.03 for either NAD^+ or L-malate. This is consistant with the linear character of the double-reciprocal plots in this direction with S-MDH *b*. However, values of the Hill coefficient obtained with S-MDH *a* and L-malate as the variable substrate were significantly greater than one. When these coefficients were examined at different values of the fixed substrate, NAD^+, it could be observed that the degree of cooperativity was dependent on the concentration of NAD^+ (Table I). A similar dependence of the Hill coefficient on the fixed substrate concentration could also be observed with S-MDH *a* and oxaloacetate as varying substrate, and with NADH and S-MDH *b* (Table I). Further, examination of the plots with varying oxaloacetate and S-MDH *b* as enzyme (Figure 5) shows that the biphasic curve observed at high fixed NADH concentrations was altered so that only downward curvature was observed at lower values of fixed NADH concentration.

Any mechanistic scheme used to interpret the kinetic data reported here must take into consideration both the curvature of the reciprocal plots, and the effect of other substrates on this curvature. The alternative models that have been used to explain cooperative kinetics can be divided into those where either kinetic or thermodynamic events are primarily responsible for the observed cooperativity. The kinetic model requires a bireactant enzyme, where the reactants add in a random manner, and where the concentrations of enzyme–substrate complexes represent a steady-state rather than an equilibrium distribution (Sweeney and Fisher, 1968). The steady-state solution to the rate equation (Dalziel, 1958) then contains square terms for the substrate concentrations, and thus may yield nonlinear plots. If multiple binding sites for each substrate exist, these are presumed to be identical and noninteracting. The thermodynamic model requires multiple binding sites, with interactions between them such that the equilibrium binding properties are changed (Monod *et al.*, 1965; Koshland *et al.*, 1966). These interactions can then be altered by the binding of modifiers to other sites on the enzyme.

The cooperativity observed with S-MDH can be explained using either model. Thus, in S-MDH *a*, the decrease in cooperativity for L-malate and oxaloacetate at high concentrations of the appropriate coenzymes, could be interpreted as the shift from a random order of substrate addition at low concentrations of the coenzyme, to an essentially ordered addition at saturating coenzyme levels. The linearity of the reciprocal plot for NADH might be more apparent than real, since the curvature could be too slight to detect over the concentration range used. Because of the extreme complexity of the steady-state rate equation for random substrate addition (Dalziel, 1958), it is essentially impossible to predict the precise form of the nonlinearity in such a mechanism unless some of the rate constants are either known or assumed. Cleland (1970) has stated that simulation studies with this mechanism, using "realistic" values for the rate constants, have generated only very slight curvature. Nevertheless, the possibility of the random-order mechanism producing nonlinear reciprocal plots cannot be neglected.

The effects observed with S-MDH *a* can equally well be explained using an interaction model. Ultracentrifuge studies suggested that S-MDH *a* exists in a monomer–dimer equilibrium, and that largely monomer will be present in solution at the concentrations used for the kinetic studies (Cassman and Vetterlein, 1974). The NAD^+ dependence of the cooperativity of L-malate kinetics could therefore arise from an NAD^+-mediated shift in polymeric states, where the affinity of the polymeric forms for L-malate differ.

The complex cooperativity exhibited by S-MDH *b* for NADH and oxaloacetate is particularly intriguing. A plot of Hill coefficients which go from 1.0 through a maximum and back to 1.0 has been defined by Rubin and Changeux (1966) in terms of the allosteric model of Monod *et al.* (1965). The appearance of a maximum in the Hill coefficients for NADH can similarly be interpreted as an induced shift by oxaloacetate between conformational states with different affinities for NADH, where the affinities in both states are nonzero. Ultracentrifuge and equilibrium binding studies with NADH had previously indicated that S-MDH *b* exists in a monomer–dimer equilibrium, with the dimer having a smaller affinity for NADH than the monomer (Cassman and King, 1972). As with S-MDH *a*, the association constant for the monomer–dimer equilibrium would suggest that S-MDH *b* exists primarily as the monomer at the concentrations used in the kinetic studies. The effect of the allosteric modifier, oxaloacetate, might also be coupled to a change in the polymeric state of the enzyme.

The reciprocal plots at high fixed NADH concentrations are rather unusual, although they have also been observed with several other bireactant and allosteric enzymes (Corwin and Fanning, 1968; LeJohn and Jackson, 1968; Levitzki and Koshland, 1969; Schutz *et al.*, 1972). Teipel and Koshland (1969) have interpreted this type of plot as being the result of interactions between more than two binding sites, where the initially identical affinities vary with substrate concentration, but where the change cannot be represented by a monotonic increase or decrease in affinity. Since S-MDH binds 1 mol of NADH/subunit, and the maximum degree of polymerization observed with or without added NADH is the dimer (Cassman and King, 1972), a model of the type described by Teipel and Koshland cannot be applicable. A comparison of the kinetic plots for oxaloacetate and NADH suggest, rather, that oxaloacetate may increase the affinity for NADH, acting thereby as a positive effector. At fixed nonsaturating NADH concentrations this would result in an apparent "substrate activation" by oxaloacetate, with the reciprocal plot with varying oxaloacetate showing downward curvature. At the highest oxaloacetate concentrations, the transition would be complete, and the reciprocal plot would then become linear with increasing oxaloacetate concentration. A computer simulation is being developed to determine whether the kinetic data can be fit quantitatively by such a model.

It should be noted that the model just described cannot be easily distinguished from a kinetic model with a random order of substrate addition. The major distinction lies in the necessity of a coupled polymerization in the thermodynamic model. Again, owing to the complexity of the rate equation for the random-order steady-state mechanism, it is difficult to determine whether a quantitative fit to the observed kinetic patterns would in fact be possible. Experimental and theoretical tests of these models are currently in progress.

Previous initial-rate kinetic studies on a beef heart MDH preparation were performed by Cassman and Englard (1966), at pH 8.5. The results indicated an ordered sequence of substrate binding for NAD^+ and L-malate, while the mechanism with NADH and oxaloacetate as substrates was not as clear-cut, and suggested a possible random-order component. Measurements at equilibrium, performed by Silverstein and Sulebele (1969a), at pH 8.0, suggested only an ordered sequence of addition in both reaction directions. There is, of course, no indication in either of these studies of the form of the S-MDH being examined. Application of these earlier results to the data

presented in this paper is further complicated by the fact that they were performed at pH 8.0–8.5, compared to pH 6.0 in the current work. It has been previously observed both with lactic dehydrogenase (Silverstein and Boyer, 1964), and with a mitochondrial malic dehydrogenase (Silverstein and Sulebele, 1969b), that a shift in pH from pH 8 to 9–9.7 causes an apparent change in the kinetic mechanism from ordered to partially ordered. Further, Cassman and Englard (1966) and Cassman (1967) have described a pH-dependent transition, centered at pH 7–7.5, in the kinetics of an S-MDH preparation. It does not, therefore, appear justifiable to make any assumptions about the kinetic mechanism(s) of S-MDH *a* or *b* at pH 6, based on the results of these previous published studies.

Any interpretation of these molecular events in terms of *in vivo* physiological mechanisms must be qualified by the recognition that different *in vivo* conditions might significantly affect key kinetic properties. However, an analysis can be undertaken assuming that qualitative and comparative properties of the enzymes reflect stable functional traits. Even with this assumption, determination of the physiological roles of S-MDH *a* and *b* remains a difficult task, since the position of S-MDH in intermediary metabolism has never been precisely defined.

Two major metabolic roles have been attributed to S-MDH. Lardy *et al.* (1965) have suggested that S-MDH may be involved in gluconeogenesis through the oxidation of cytoplasmic L-malate to oxaloacetate, which is then converted to phosphoenolpyruvate. This is unlikely to be significant in heart muscle, a tissue that does not appear to carry out gluconeogenesis to any significant extent (Scrutton and Utter, 1968). S-MDH has also been implicated in the reoxidation of cytoplasmic NADH generated in glycolysis (Krebs *et al.*, 1967). The malate produced is assumed to be actively transported into the mitochondria and reoxidized by mitochondrial MDH. The oxaloacetate would then be transported back to the cytoplasm either through direct transport, or as aspartate, coupled to aspartate transminase, an enzyme found in both mitochondria and cytoplasm (Boyd, 1961). A possible alternative shuttle mechanism for the reoxidation of glycolytic NADH, involving glycerophosphate dehydrogenase, is unlikely to occur in heart muscle because of the low levels of the enzymes required (Haslam and Krebs, 1968).

Since the reoxidation of cytoplasmic NADH can also be accomplished by lactic dehydrogenase, some mechanism must exist which would regulate the flow of reducing equivalents to lactate or to the mitochondria. The molecular properties of S-MDH *a* and *b* are consistent with the physiological requirements for such a regulatory mechanism. S-MDH *b* has a kinetic behavior which permits a sensitive response to varying oxaloacetate levels. The apparent substrate activation of S-MDH *b* with increasing oxaloacetate concentrations and the allosteric behavior of NADH allow a ready adjustment of the rate to changing substrate levels. In addition, fructose 1,6-bisphosphate has been shown to allosterically inhibit NADH binding to S-MDH *b* (Cassman, 1973), and inhibit the rate of NADH oxidation (M. Cassman, unpublished observations). This effect might help to explain the funneling of reducing equivalents to lactate under anaerobic conditions, where an increased glycolytic rate is paralleled by an increase in fructose bisphosphate levels (Williamson, 1966).

S-MDH *a*, however, shows only little cooperative interactions in the direction of NADH oxidation, and is completely insensitive to added fructose diphosphate (Cassman and Vetterlein, 1974). The maximum rate of NADH oxidation with S-MDH *a* is three times higher than that with S-MDH *b*, and the dissociation constant for NADH is approximately one-half that of S-MDH *b* (Cassman and Vetterlein, 1974). All of this suggests that the fructose bisphosphate effect and cooperative interactions of oxaloacetate and NADH with S-MDH *b* constitute a fine control system on the oxidation of NADH. The mechanism which operates to convert S-MDH *b* to S-MDH *a* would then represent a superimposed control which generates an enzyme species markedly less susceptible to allosteric controls on NADH utilization, and with kinetic and binding properties which further increase the capacity of the enzyme to catalyze the oxidation of NADH. The significance of the cooperativity of S-MDH *a* with respect to L-malate is not clear.

The major structural difference between S-MDH *a* and *b* is the amount of covalently bound phosphate, with S-MDH *a* containing 0.65–0.90 mol of phosphate/subunit, while S-MDH *b* contains 0.10–0.30 mol of phosphate/subunit (Cassman and Vetterlein, 1974). A comparison immediately suggests itself with other phospho-dephosphoenzymes involved in glycolysis. Both phosphorylase and glycogen synthetase have active and inactive (or, more properly, less active) enzyme forms which are interconverted by covalent addition or removal of phosphate (Fischer and Krebs, 1955; Friedman and Larner, 1961). In these enzymes, as in S-MDH, the "inactive" form shows markedly greater allosteric responses than does the "active" form (Helmreich, 1969; Mersman and Segal, 1967). Whether S-MDH *a* and *b* are interconverted by similar mechanisms will require further investigation.

References

Alberty, R. A. (1953), *J. Amer. Chem. Soc. 75,* 1928.

Boyd, J. W. (1961), *Biochem. J. 81,* 434.

Burton, K., and Wilson, T. H. (1953), *Biochem. J. 54,* 86.

Cassman, M. (1967), *J. Biol. Chem. 242,* 2013.

Cassman, M. (1973), *Biochem. Biophys. Res. Commun. 53,* 666.

Cassman, M., and Englard, S. (1966), *J. Biol. Chem. 241,* 793.

Cassman, M., and King, R. C. (1972), *Biochemistry 11,* 4937.

Cassman, M., and Vetterlein, D. (1974), *Biochemistry 13,* 684.

Cleland, W. W. (1970), *Enzymes 2,* Chapter 1.

Corwin, L. M., and Fanning, G. K. (1968), *J. Biol. Chem. 243,* 3517.

Dalziel, K. (1957), *Acta Chem. Scand. 11,* 1706.

Dalziel, K. (1958), *Trans. Faraday Soc. 54,* 1247.

Dolin, M. I. (1968), *J. Biol. Chem. 243,* 3916.

Fischer, E. H., and Krebs, E. G. (1955), *J. Biol. Chem. 216,* 121.

Frieden, C. (1967), *J. Biol. Chem. 242,* 4045.

Friedman, D. L., and Larner, J. (1963), *Biochemistry 2,* 669.

Guha, A., Englard, S., and Listowsky, I. (1968), *J. Biol. Chem. 243,* 609.

Haslam, J. N., and Krebs, H. A. (1968), *Biochem. J. 107,* 659.

Helmreich, E. (1969), *Fed. Eur. Biochem. Soc. Symp. 19,* 131.

Holzer, H., and Duntze, W. (1971), *Annu. Rev. Biochem. 40,* 345.

Horecker, B. L., and Kornberg, A. (1949), *J. Biol. Chem. 175,* 385.

Koshland, D. E., Jr., Nemethy, G., and Filmer, D. (1966), *Biochemistry 5,* 365.

Krebs, H. A., Gascoyne, T., and Notton, B. (1967), *Biochem. J. 105,* 275.

Lardy, H. A., Paetku, V., and Walter, P. (1965), *Proc. Nat. Acad. Sci. U. S. 53,* 1410.

LeJohn, H. B., and Jackson, A. (1968), *J. Biol. Chem. 243,* 3447.

Levitzki, A., and Koshland, D. E., Jr. (1969), *Proc. Nat. Acad. Sci. U. S. 62,* 1121.

Loewus, F. A., Tchen, T. T., and Vennesland, B. (1955), *J. Biol. Chem. 212*, 787.

Mersman, H. J., and Segal, H. L. (1967), *Proc. Nat. Acad. Sci. U. S. 58*, 1688.

Monod, J., Wyman, J., and Changeux, J.-P. (1965), *J. Mol. Biol. 12*, 68.

Plowman, K. M. (1972), Enzyme Kinetics, New York, N. Y., McGraw-Hill Book Co.

Rubin, M. M., and Changeux, J.-P. (1966), *J. Mol. Biol. 21*, 265.

Schutz, G., Chow, E., and Feigelson, P. (1972), *J. Biol. Chem. 247*, 5333.

Scrutton, M. C., and Utter, M. F. (1968), *Annu. Rev. Biochem. 37*, 249.

Silverstein, E., and Boyer, P. D. (1964), *J. Biol. Chem. 239*, 3901.

Silverstein, E., and Sulebele, G. (1969a), *Biochim. Biophys. Acta 185*, 297.

Silverstein, E., and Sulebele, G. (1969b), *Biochemistry 8*, 2543.

Sweeney, J. R., and Fisher, J. R. (1968), *Biochemistry 7*, 561.

Teipel, J., and Koshland, D. E., Jr. (1969), *Biochemistry 8*, 4656.

Whitehead, E. (1970), *Progr. Biophys. Mol. Biol. 20*, 321.

Williamson, J. R. (1966), *J. Biol. Chem. 241*, 5026.

Rates of Peptide-Bond Hydrolysis by Cobalt(III) Complexes†

S. K. Oh and C. B. Storm*

ABSTRACT: The rates of hydrolysis of the peptides Gly-Gly, Gly-L-Leu, Gly-L-Tyr, Gly-D,L-Val, Gly-L-Try, L-Ala-L-Phe, D,L-Leu-Gly, L-Pro-L-Tyr, L-Val-Gly, and L-Val-L-Ile have been determined using the Co(III)(trien)(OH)$(H_2O)^{2+}$ and the Co(III)(edda)(OH)(H_2O) complexes. The rate of hydrolysis of the reduced, carboxymethylated insulin A chain by the Co(III)(edda)(OH)(H_2O) has also been determined. With the trien complex the rates of hydrolysis vary from 0.25 l. mol^{-1} sec^{-1} for Gly-Gly to 0.022 l. mol^{-1} sec^{-1} for L-Val-L-Ile, giving a maximum variation of rate of 11.9. With the edda complex the rates of hydrolysis vary from 0.13 l. mol^{-1} sec^{-1} for Gly-L-Tyr to 0.016 l. mol^{-1} sec^{-1} for L-Val-Gly, giving a maximum variation of rate of 8.5. This compares to a rate variation of over 100 for the acid hydrolysis of these same peptides. Under pseudo-first-order conditions the rate of hydrolysis of the reduced, carboxymethylated insulin A chain by the edda complex is linear and the rate is essentially the same as with the model peptides. These data demonstrate that these reagents are suitable for use in sequencing proteins.

Methods of protein degradation and amino acid analysis that do not in any way alter or destroy any of the naturally occurring amino acids would be of considerable use in protein structure determination. Such a potential method was described by Collman and Buckingham (1963) when they demonstrated that Co(trien)(OH)$(H_2O)^{2+}$ [1] hydrolyzed peptides stoichiometrically from the N-terminal end under mild conditions of pH and at moderate temperatures. Since that time a number of similar systems have been reported. The complex Co$(en)_2$(OH)$(H_2O)^{2+}$ undergoes competing side reactions limiting its utility (Buckingham and Collman, 1967). The Co(tren)(OH)$(H_2O)^{2+}$ complex shows a somewhat greater N-terminal selectivity than the trien complex and reacts at a slower rate (Kimura *et al.* 1970). Worrell and Busch (1969) have reported that the Co(eee)(OH)$(H_2O)^{2+}$ also hydrolyzes both amide and ester bonds. The Co(edda)(OH)(H_2O) complex acts in a similar manner to the trien complex; however, the pH of its maximum rate is more basic (Oh and Storm, 1973).

There have been a number of investigations of the mechanism of the metal ion promoted amide and ester bond hydrolysis by the cobalt tetramine complexes (Buckingham *et al.*, 1970a,c; Wu and Busch, 1970). The mechanism for the peptide-bond hydrolysis by the Co(trien)(OH)$(H_2O)^{2+}$ system involves the replacement of a coordinated water molecule by the terminal amino group of the peptide, as the rate-determining step, followed by rapid hydrolytic cleavage of the peptide bond. The peptide-bond cleavage can involve either activation of the carbonyl group through coordination to the cobalt center or attack on the carbonyl group by the adjacent coordinated hydroxide group (Buckingham *et al.*, 1967, 1969). The rates of peptide-bond hydrolysis observed using these complexes are some 10^4–10^7 faster than observed for the free peptide (Hay and Morris, 1969; Buckingham *et al.*, 1970b). The important effect in the rate acceleration is evidently the template effect (Jencks, 1969).

The concepts involved in using these Co(III) reagents in amino acid analysis and sequencing are identical with those involved in using leucine aminopeptidase and have been discussed by Light (1967). For sequencing studies the critical factor is the relative rate at which various residues are cleaved. With leucine aminopeptidase the rates vary widely, due to enzymic specificity, and the leucine aminopeptidase hydrolysis of proteins has met with limited use in sequencing work. There are two reports in the literature concerning a high degree of selectivity with cobalt tetramine complexes (Girgis and Legg, 1972; Kistenmacher *et al.*, 1973). The use of the trien complex

† From the Department of Chemistry, Howard University, Washington, D. C. 20001. *Received November 27, 1973.* This work has been supported by grants from the National Institutes of Health (GM 18552) and the Research Corporation.

*Recipient of Public Health Service Career Development Award GM-70586 from the National Institute of General Medical Sciences.

[1] Abbreviations used are: en, ethylenediamine; trien, triethylenetetramine; tren, 2′,2″,2‴-triaminotriethylenetetramine; edda, ethylenediaminediacetato; eee, 1,8-diamino-3,6-dithiaoctane; AA, amino acid anion; the common symbols for the amino acids are used.